Unary Coding Controlled Simultaneous Wireless Information and Power Transfer in Binary Symmetric Channel

Jie Hu, *Member, IEEE*, Mengyuan Li, Kai-Kit Wong, *Fellow, IEEE*,

Kun Yang, *Senior Member, IEEE*

Abstract

Due to its long-range propagation nature, radio frequency (RF) signals have been relied upon for both the wireless information delivery and the wireless charging to the massively deployed low-power devices in the upcoming era of Internet of Things (IoT). Therefore, intensive efforts have been invested in the physical layer and the medium-access-control layer design for coordinating simultaneous wireless information and power transfer (SWIPT) in the RF band. Distinguished from the existing works, we study the coding-level control controlled SWIPT from the information theoretical perspective in a classic binary symmetric channel. Due to its practical decoding implementation and its flexibility on the codeword structure, the unary code is chosen as a joint information and energy encoder. The wireless power transfer performance in terms of the energy carried per bit and of the battery underflow/overflow probability is maximised by optimising the codeword distribution of the unary code, while satisfying the require wireless information transfer (WIT) performance in terms of the mutual information. Furthermore, the

Jie Hu, Mengyuan Li and Kun Yang are with the School of Information and Communication Engineering, University of Electronic Science and Technology of China, Chengdu, China, 611731, email: hujie@uestc.edu.cn, 201721010518@std.uestc.edu.cn, kunyang@uestc.edu.cn.

Kai-Kit Wong is with the Department of Electronic and Electrical Engineering, University College London, UK, WC1E 6BT, email: kai-kit.wong@ucl.ac.uk.

Genetic Algorithm (GA) aided coding design is proposed to reduce the computational complexity. The numerical results characterise the SWIPT performance and validate the optimality of our proposed GA aided unary coding design.

Index Terms

SWIPT, unary coding, binary symmetric channel, mutual information, energy per bit and battery overflow/underflow probability

I. Introduction

In the upcoming era of Internet of Things (IoT), massively deployed low-power devices may swallow a major portion of the wireless communication throughput [1]. All functions of these IoT devices, such as the data collection, data processing, data downloading and data uploading are powered by their embedded batteries [2]. Frequent operations may quickly drain the batteries having limited capacity. However, a lot of IoT devices are deployed in hardly reachable places. Replacing the batteries or even replacing the IoT devices is a cumbersome task for the network operator, which may substantially increase their operating expense.

Therefore, the network operators continuously seek for an economic way to recharging their IoT devices. Some IoT devices are enabled to harvesting energy from renewable sources [3], such as sunlight, wind, tide and sporadic radio frequency (RF) signals. However, the stochastic arrival of the renewable energy imposes challenges on the design of the communication strategies [4]. For example, the optimal transmit power control should be re-designed by considering the energy causality induced by the stochastic energy arrival. Hence, the operator prefers a controllable and reliable remote charging paradigm to reduce the uncertainty of the renewable energy harvesting.

RF signal based wireless power transfer (WPT) beats its near-field counterparts[1] as a promising

[1]Inductive coupling [5] and magnetic resonance based WPT [6] techniques can only transfer power to the near-field devices, which are only several millimetres or centimetres away from the WPT transmitter.

paradigm to recharge the IoT devices for the following reasons:

- It may transfer wireless power to the far-field IoT devices[2];
- It may flexibly form a narrow-beam to charge a single device and form a wide-beam to charge multiple devices;
- Sufficient legacy RF signal transmitters exist, which results in low investment on the WPT infrastructure.

However, wireless information transfer (WIT) has already resided in the RF band. Introducing the WPT in the same spectral band may severely degrade WIT performance, since they may compete for the precious radio resources to fulfil their distinctive targets. Therefore, careful coordination of both WIT and WPT in the RF band is required for simultaneously satisfying the devices communication and charging demands, which yields an emerging technique of simultaneous wireless information and power transfer (SWIPT) [7].

Intensive endeavours have been invested in SWIPT spanning from the signal design and the transceiver design to the medium-access-control strategy as well as resource allocation and networking scheme [8]–[12], [12]–[16]. For example, Clerckx *et al.* [8] designed the optimal multi-sinusoidal signal for the dedicated WPT, while Y. Zeng *et al.* [9] focused on the design of the multi-sinusoidal SWIPT signal. Zhou et al. [10] made the very first contribution to the receiver arhictecture of SWIPT, which adopted either a power splitter, a time switcher or a current splitter for simultanous reception of the information and energy. Moreover, Zhang *et al.* [11] optimised transmit beamformer for the MIMO aided SWIPT transmitter. Furthermore, Lv *et al.* [12] proposed an optimal time-domain resource allocation schemes for the time-division-multiple-access (TDMA) aided multi-user SWIPT system, which aims for maximising the sum-throughput and the fair-throughput of the users' uplink transmission, respectively. Based on

[2]Normally, RF signals are capable of transferring wireless power to the IoT devices several metres away. If the transmit power is sufficiently high, we may transfer wireless power several kilometres away.

[12], Yang *et al.* introduced the multiple antenna to the SWIPT transmitter, which results in joint resource allocation schemes [13] in the spatial-, time- and power-domain. In order to support the “ad hoc” access of the batteryless devices, Zhao *et al.* proposed several enhanced carrier-sensing-multiple-access and collision avoidance (CSMA/CA) protocols and analyse their attainable performance in [14] and [15]. Furthermore, Zhao *et al.* [16] also studied the optimal deployment scheme of the SWIPT transmitters by considering the social characteristics of the mobile SWIPT users.

Surprisingly, the research on the information theoretical essence of the SWIPT has not become prosperous, since Varshney [17] firstly studied the tradeoff between the maximum mutual information and the energy harvesting requirement in different channels. This seminal work demonstrated that the performance of the SWIPT can be controlled by adjusting the codeword structure, which provides the theoretical fundamental for the coding controlled SWIPT. Furthermore, Varshney [18] also proposed a cross-layer architecture for jointly optimising both the energy and information delivery from the information theoretical perspective, where a powerline communication system was exemplified as a typical integrated information and energy transfer system. Moreover, Tandon *et al.* [19] divided a codeword into several sub-blocks for satisfying the receiver’s real-time energy demands. The optimal structure of the codeword is found for maximising the mutual information in a binary symmetric channel (BSC). However, both of [17] and [19] only considered memoryless information source in their analysis but ignored the correlation among the bits in the output sequence of a practical encoder. Therefore, these works optimised the transmit probabilities of the binary bits in order to achieve the maximum SWIPT performance without considering a practical coding scheme.

The conventional source encoders generates equi-probable binary bits for maximising the codewords’ capability of the information transmission. However, the codewords having equi-probable binary bits are only capable of carrying a fixed amount of energy. Therefore, the conventional source encoder cannot satisfy the diverse energy requests of the receiver. The *constrained code* [20] has a certain degree of freedom to adjust the codeword structure for satisfying the WPT requirement without sacrificing the WIT efficiency.

As a typical constrained code, a run-length-limited (RLL) encoder was designed by Fouladgar *et al.* [21] for minimising the battery overflow/underflow probability at the receiver subject to the constraint on the achievable mutual information. Moreover, Tandon *et al.* [22] found the lower-bound of the capacity of the BSC and Z channel, when the (d, ∞) RLL code was adopted. However, they only use the minimum run-length d to ensure the minimum energy delivery requirement, which largely overlook the devices' long-term energy requirements.

Furthermore, unary code has been widely used for the source coding [23]–[25] in wireless communication, due to its low encoding and decoding complexity. Specifically, the unary code was used by Babar *et al.* [23] for the joint throughput and dimming control in the visible light communication system. However, the SWIPT performance of the unary code in the RF band has not been studied from the information theoretical perspective.

Against this background, our novel contributions are summarised as below:

- *We propose a practical unary coding aided SWIPT transceiver and analysed its performance from the information theoretical perspective. The correlation among the information bits generated by the unary encoder has been taken into account in the performance analysis.*
- *By considering the infinite battery capacity, the optimal codeword distribution is found for maximising the average energy carried by a single output bit of the BSC, while satisfying the mutual information requirement.*
- *By considering the finite battery capacity, the optimal codeword distribution is also found for minimising the battery overflow/underflow probability of the receiver, while satisfying the mutual information requirement.*
- *The optimal coding design is obtained by exploiting a low-complexity Genetic Algorithm*

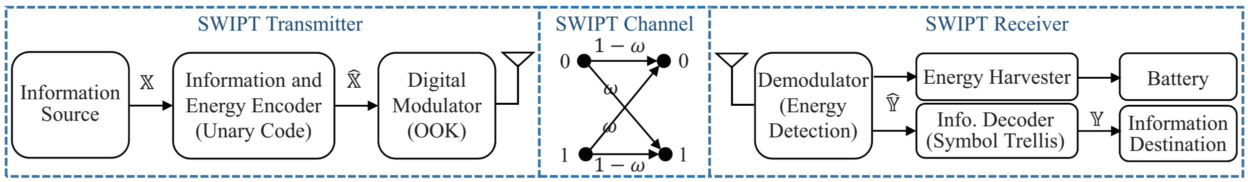

Fig. 1. The transceiver architecture of a single-user SWIPT system.

(GA), which achieves almost the same performance of the exhaustive searching (ES).

The rest of the paper is organised as follows: the system model of the unary coding aided SWIPT transceiver is introduced in Section II. The WIT performance is then analysed in Section III, which is followed by the WPT performance analysis in Section IV. After formulating and solving the optimal coding design problem in Section V, numerical results are illustrated in Section VI. Finally, our paper is concluded in Section VII.

II. System Model

A. SWIPT Transmitter

The architecture of a SWIPT transmitter is portrayed in Fig.1, which is constituted by the following functional modules:

- *Information Source* $\mathbb{X}$ outputs the messages randomly chosen from the message book $\boldsymbol{\mathcal{X}} = \{\mathcal{X}_1, \cdots, \mathcal{X}_K\}$.
- *Information and Energy Encoder* encodes the messages into binary codewords, which can be regarded as the coded source $\widehat{\mathbb{X}}$. We adopt the unary encoder for mapping the j-th message $\mathcal{X}_j$ onto a j-bits codeword $\widehat{\mathcal{X}}_j$ having $(j-1)$ bit '1' followed by a single bit '0'. The K-level unary code provides K different codewords, as portrayed in TABLE I.
- *Digital Modulator* modulates the binary codewords onto the analogue RF signals. Amplitude based modulator allocates different power to the codewords. In order to highlight the impact of the codeword structure on the SWIPT performance, we adopt the on-off-keying (OOK)

TABLE I
K-LEVEL UNARY CODE

Messages	Codewords	Codeword Prob.	Energy
$\mathcal{X}_1$	$\widehat{\mathcal{X}}_1 = 0$	$p(\widehat{\mathcal{X}}_1)$	$g(\widehat{\mathcal{X}}_1) = 0$
$\mathcal{X}_2$	$\widehat{\mathcal{X}}_2 = 10$	$p(\widehat{\mathcal{X}}_2)$	$g(\widehat{\mathcal{X}}_2) = \frac{1}{2}$
$\mathcal{X}_3$	$\widehat{\mathcal{X}}_3 = 110$	$p(\widehat{\mathcal{X}}_3)$	$g(\widehat{\mathcal{X}}_3) = \frac{2}{3}$
$\vdots$	$\vdots$	$\vdots$	$\vdots$
$\mathcal{X}_K$	$\widehat{\mathcal{X}}_K = \underbrace{11\cdots 1}_{(K-1)\text{ bit}}0$	$p(\widehat{\mathcal{X}}_K)$	$g(\widehat{\mathcal{X}}_{2^k}) = \frac{K-1}{K}$

based digital modulator. Bit '1' is represented by the presence of the RF signal $A\sin(2\pi f t)$, where A and f denotes its amplitude and frequency, respectively. When bit '1' is transmitted, the amount of energy carried by its modulated RF signal is expressed as

$$E(1) = \int_0^T A^2 \sin^2(2\pi f t) dt = \frac{A^2}{2} - \frac{A^2}{8\pi f}\sin(4\pi f T), \tag{1}$$

where T is the duration of the modulated symbol. Furthermore, bit '0' is represented by the absence of the RF signal. Its energy is thus $E(0) = 0$. Therefore, the energy carried by a codeword is determined by its number of bit '1'.

B. SWIPT Receiver

The following modules are implemented at the SWIPT receiver for information recovery, as illustrated in Fig.1:

- *Digital Demodulator* demodulates the information carried by the received RF signal. We implement the energy detector to demodulate the RF signal modulated by OOK. The resultant binary bit sequences constitute the coded destination $\widehat{\mathbb{Y}}$.
- *Information Decoder* decodes the received codeword in order to recover the original message. The symbol-level trellis can be invoked for efficiently decoding the unary codeword [23]–[25], which is capable of avoiding the catastrophic error propagation.
- *Information Destination* receives the recovered message, which is denoted as $\mathbb{Y}$.

Similar to [17], [19], [21]–[23], we consider an ideal SWIPT receiver, in which the RF signal flows into the digital demodulator may be reused for energy harvesting. The following modules are implemented at the SWIPT receiver for energy harvesting:

- *Energy Harvester* converts the RF signal received by the antenna to the direct current (DC).
- *Battery* is charged by the DC. We consider batteries having both infinite and finite capacity in the optimal coding design.

C. SWIPT Channel

The impact of the channel attenuation between a transmitter and receiver pair can be modelled by a BSC, as portrayed in Fig.1:

- When a bit '0' is transmitted, the receiver may successfully receive bit '0' with a probability of $(1 - \omega)$, if the power of the accumulated noise and the ambient RF signal is lower than the threshold of the energy detector, which also indicates no energy is harvested by the receiver. Otherwise, the receiver may erroneously receive bit '1' with a probability of ω, which also indicates that the receiver may harvest a single unit of energy from the ambient RF signal and the noise.
- When a bit '1' is transmitted, the modulated RF signal may be severely attenuated by the wireless channel. The accumulated power of the received modulated RF signal, the ambient RF signal and the noise may be lower than the threshold of the energy detector, which may result in the erroneous reception of bit '0' and the failure WPT. This event may happen with a probability of ω. By contrast, the successful reception of bit '1' and the successful WPT can be achieved with a probability of $(1 - \omega)$, if the power of the accumulated signal received is still higher than the energy detection threshold.

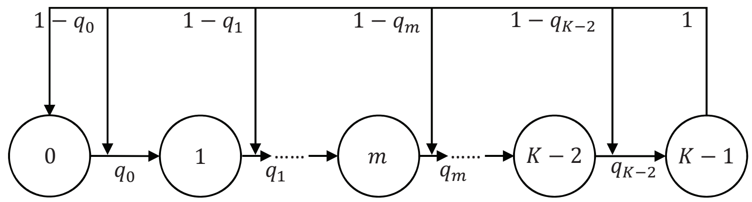

Fig. 2. Markov modelling of the unary coded information source.

III. WIT Performance Analysis

We firstly analyse the WIT performance in terms of the lower bound of the SWIPT channel's mutual information.

A. Markov Modelling

The K-level unary encoded transmitter sends an arbitrary codeword chosen from the codebook $\widehat{\boldsymbol{X}} = \{\widehat{X}_1, \widehat{X}_2, \cdots, \widehat{X}_K\}$ for conveying both information and energy to the receiver, as shown in TABLE I. The probabilities of these codewords being sent are denoted by $\mathbf{P} = \{p(\widehat{X}_1), p(\widehat{X}_2), \cdots, p(\widehat{X}_K)\}$. Sequentially sending a range of unary codewords generates a N-bit sequence $\mathbf{X}_N = \{X_1, X_2, \cdots, X_N\}$. The correlation among the binary bits can be modelled by a finite-state Markov chain, as illustrated in Fig.2.

State m of this Markov chain represents that we currently have a run of bit '1' having a length of m. As presented in TABLEI, the maximum allowable run-length of bit '1' is $(K-1)$ for a K-level unary code. Therefore, the Markov chain of Fig.2 spans from state 0 to $K-1$. The state transition from m to $(m+1)$ occurs with a probability of q_m, if an additional bit '1' is output by the encoder. The output of a bit '0' terminates the current run of bit '1', which results in a state transition from m back to 0 with a probability of $(1-q_m)$. A state sequence $\mathbf{S}_N = \{S_1, S_2, \cdots, S_N\}$ can be mapped onto the bit sequence $\mathbf{X}_N = \{X_1, X_2, \cdots, X_N\}$, as portrayed in Fig.3. For an example of a 4-level unary code, a 6-states sequence $\mathbf{S}_6 = \{1, 2, 0, 1, 2, 3, 0\}$ corresponds to a bit sequence $\mathbf{X}_6 = \{1, 1, 0, 1, 1, 1, 0\}$.

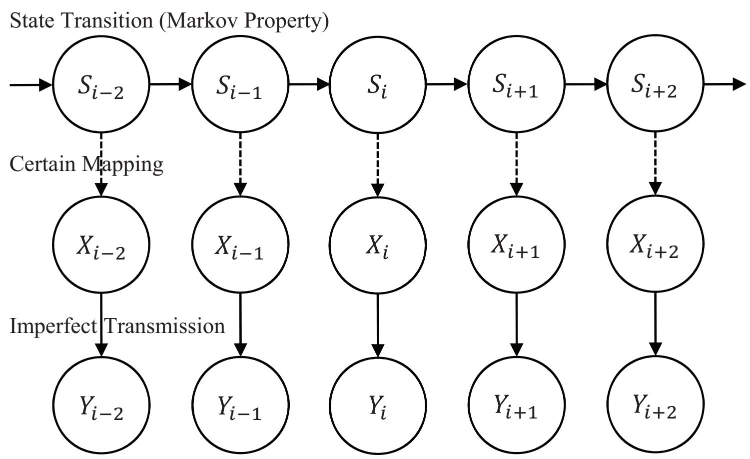

Fig. 3. Correlation among the state sequence and the bit sequences of the channel input/output.

The state transition probability q_m is a function of the codeword distribution $\mathbf{P}$, which is formulated as:

$$q_m = 1 - p(\widehat{X}_1) - p(\widehat{X}_2) - \cdots - p(\widehat{X}_{m+1}), \tag{2}$$

for $0 \leq m \leq K-1$. The matrix $\mathbf{Q}$ of the state transition probabilities is expressed as:

$$\mathbf{Q} = \begin{bmatrix} 1-q_0 & q_0 & 0 & \cdots & 0 & 0 \\ 1-q_1 & 0 & q_1 & \cdots & 0 & 0 \\ \vdots & \vdots & \vdots & \ddots & \vdots & \vdots \\ 1-q_{K-2} & 0 & 0 & \cdots & 0 & q_{K-2} \\ 1 & 0 & 0 & \cdots & 0 & 0 \end{bmatrix}. \tag{3}$$

The stationary distribution $\boldsymbol{\pi} = \{\pi_0, \pi_1, \cdots, \pi_{K-1}\}$ of the Markov chain can be obtained by solving the following linear equations:

$$\begin{cases} \boldsymbol{\pi} \times \mathbf{Q} = \boldsymbol{\pi} \\ \boldsymbol{\pi} \times \mathbf{I}_{K\times 1} = 1 \end{cases}, \tag{4}$$

where $\mathbf{I}_{K\times 1}$ is a $K \times 1$ column vector having all its entries equal to one. Both $\boldsymbol{\pi}$ and $\mathbf{Q}$ are essential for calculating the mutual information.

B. Mutual Information

When the N-bit sequence $\mathbf{X}_N$ is input to the channel, the corresponding output bit sequence is $\mathbf{Y}_N = \{Y_1, Y_2, \cdots, Y_N\}$ after the imperfect transmission, as exemplified in Fig.3. The mutual information between the coded source $\widehat{\mathbb{X}}$ and the coded destination $\widehat{\mathbb{Y}}$ can be formulated as

$$I(\widehat{\mathbb{X}}; \widehat{\mathbb{Y}}) = H(\widehat{\mathbb{X}}) - H(\widehat{\mathbb{X}}|\widehat{\mathbb{Y}}). \tag{5}$$

The entropy $H(\widehat{\mathbb{X}})$ of the coded source can be expressed as

$$\begin{aligned} H(\widehat{\mathbb{X}}) = \lim_{N\to\infty} \frac{H(\mathbf{X}_N)}{N} &\overset{(a)}{=} \lim_{N\to\infty} \frac{H(\mathbf{S}_N)}{N} \\ &\overset{(b)}{=} \lim_{N\to\infty} H(S_N|S_1, S_2, \cdots, S_{N-1}) \\ &\overset{(c)}{=} \lim_{N\to\infty} H(S_N|S_{N-1}) \\ &\overset{(d)}{=} H(S_2|S_1). \end{aligned} \tag{6}$$

In Eq.(6), the equality (a) is derived due to the certain mapping between the bit sequence $\mathbf{X}_N$ and the state sequence $\mathbf{S}_N$, as exemplified in Fig.3. The equality (b) is obtained by exploiting *Theorem 4.2.1* of [26]. The equality (c) is derived due to the Markov property of the unary coded information source, while the derivation of the equality (d) is based on the stationary property of the coded source $\mathbb{X}$.

Observe from Fig.3 that the state sequence $\mathbf{S}_N$ is also correlated to the bit sequence $\mathbf{Y}_N$ of the channel output. In order to obtain the conditional entropy $H(\widehat{\mathbb{X}}|\widehat{\mathbb{Y}})$, the following pair of Lemmas are introduced for investigating the correlation between $\mathbf{S}_N$ and $\mathbf{Y}_N$:

Lemma 1: Given state S_i at the i-th instant, state S_{i+1} is independent of the channel output bits $\{Y_1, \cdots, Y_{i-1}, Y_i\}$ at the previous instants.

Proof: The Markov chain transits from state S_i to S_{i+1} by sticking to the encoding principle of the unary code. By contrast, the transition from state S_i to bit Y_i is induced by the imperfect transmission in the channel. Obviously, the state transition from S_i to S_{i+1} is uncorrelated to the transition process from state S_i to bit Y_i. Given this fact, we prove the independence of S_{i+1} and Y_i in our technical report [27][3]. We then prove that $\{Y_1, \cdots, Y_{i-1}\}$ are all uncorrelated to state S_{i+1} for the following reasons: Firstly, $\{Y_1, \cdots, Y_{i-1}\}$ only depends on the states $\{S_1, \cdots, S_{i-1}\}$, respectively. Secondly, state S_{i+1} only depends on S_i but it is independent of $\{S_1, \cdots, S_{i-1}\}$, when S_i is given. ■

Lemma 2: State S_i at the i-th instant is correlated to the channel output bits $\{Y_{i+1}, Y_{i+2}, ...\}$ at the subsequent instants. If the state transition probabilities satisfy $\{q_m = q | m = 0, 1, \cdots, K-1\}$, where $q \in (0, 1)$ is a constant, S_i is independent of $\{Y_{i+1}, Y_{i+2}, \cdots\}$.

Proof: The basic principle is to find the inequalities of $\{p(S_i = s_i | Y_{i+n} = y_{i+n}) \neq p(S_i = s_i) | n = 1, 2, \cdots, \}$, where $s_i \in \{0, 1, \cdots, 2^k - 1\}$ and $y_{i+n} \in \{0, 1\}$. The sufficient condition is also found to make the equalities hold. Please refer to [27] for the detailed proof. ■

Therefore, the conditional entropy $H(\widehat{\mathbb{X}}|\widehat{\mathbb{Y}})$ is calculated as

$$
\begin{aligned}
H(\widehat{\mathbb{X}}|\widehat{\mathbb{Y}}) &= \lim_{N\to\infty} \frac{H(\mathbf{X}_N|\mathbf{Y}_N)}{N} = \lim_{N\to\infty} \frac{H(\mathbf{S}_N|\mathbf{Y}_N)}{N} \\
&\overset{(e)}{=} \lim_{N\to\infty} \frac{1}{N}\Big[H(S_1|Y_1, \cdots, Y_N) + \sum_{i=2}^{N} H(S_i|S_{i-1}, \cdots, S_1, Y_1, \cdots, Y_N)\Big] \\
&\overset{(f)}{=} \lim_{N\to\infty} \frac{1}{N}\Big[H(S_1|Y_1, \cdots, Y_N) + \sum_{i=2}^{N} H(S_i|S_{i-1}, Y_i, \cdots, Y_N)\Big] \\
&\overset{(g)}{\leq} \lim_{N\to\infty} \frac{H(S_1|Y_1, \cdots, Y_N) + (N-1)H(S_2|S_1, Y_2)}{N} \\
&= H(S_2|S_1, Y_2). \qquad (7)
\end{aligned}
$$

By exploiting the *chain rule for entropy* (*Theorem 2.5.1* in [26]), we obtain the equality (e)

[3]This technical report is also uploaded as the supplemental material of this paper

of Eq.(7). The equality (f) is derived by exploiting i) the Markov property and ii) *Lemma 1*. According to *Lemma 2*, State S_i is dependent of the channel output bits $\{Y_i, Y_{i+1}, \cdots, Y_N\}$, which results in the inequality (g).

By substituting Eqs.(6) and (7) into (5), the mutual information is further derived as

$$\begin{aligned}
I(\widehat{\mathbb{X}}; \widehat{\mathbb{Y}}) &\overset{(h)}{\geq} H(S_2|S_1) - H(S_2|S_1, Y_2) = I(S_2; Y_2|S_1) = H(Y_2|S_1) - H(Y_2|S_2, S_1) \\
&= -\sum_{s_1}\sum_{y_2} p(y_2, s_1) \log_2 p(y_2|s_1) + \sum_{s_1}\sum_{s_2}\sum_{y_2} p(y_2, s_2, s_1) \log_2 p(y_2|s_2 s_1) \\
&\overset{(i)}{=} \sum_{i=0}^{K-1} \pi_i \left\{H[q_{s_1}\omega + (1 - q_{s_1})(1 - \omega)] - H(\omega)\right\} \overset{\Delta}{=} I_{\inf}(\widehat{\mathbb{X}}; \widehat{\mathbb{Y}}),
\end{aligned} \tag{8}$$

where $H(x) = -\log_2(x) - \log_2(1 - x)$ for $0 < x < 1$. The inequality (h) of Eq.(8) is obtained by substituting the upper bound $H(S_2|S_1, Y_2)$ of the conditional entropy $H(\widehat{\mathbb{X}}|\widehat{\mathbb{Y}})$. We further derive the equality (i) by exploiting the stationary distribution $\boldsymbol{\pi}$ of the Markov chain and the corresponding matrix $\mathbf{Q}$ of the transition probabilities. The lower bound of $I(\widehat{\mathbb{X}}; \widehat{\mathbb{Y}})$ derived in Eq.(8) is attainable, according to *Lemma 2*. Therefore, it is the infimum of $I(\widehat{\mathbb{X}}; \widehat{\mathbb{Y}})$ denoted as $I_{\inf}(\widehat{\mathbb{X}}; \widehat{\mathbb{Y}})$, which is a function of the codeword distribution $\mathbf{P}$, since entries in both $\mathbf{Q}$ and $\boldsymbol{\pi}$ are functions of $\mathbf{P}$.

IV. WPT Performance Analysis

As expressed in Eq.(1), if the symbol duration T equal to the period of the RF signal, *a single energy unit* is defined as $E(1) = \frac{A^2}{2}$, when energy bit '1' is sent. The amount of energy arriving at the receiver depends on i) which codeword is transmitted, since different codewords carry different number of energy bit '1', and on ii) the imperfect transmission through the BSC, where energy bit '1' may be flipped to '0' resulting in the energy loss and bit '0' may be flipped to '1' resulting in the energy gain.

A. Infinite Battery Capacity

When the battery has an infinite capacity, we focus on the average energy carried by a single bit received by the SWIPT receiver.

When the Markov chain of Fig.2 stays at state m, the K-level unary encoder may output a bit '1' with a probability of q_m, while it may output a bit '0' with a probability of $(1 - q_m)$. Given the stationary distribution $\boldsymbol{\pi}$ derived by solving the linear equations of Eq.(4), the stationary probability of the encoder outputting a bit '1' can be calculated by $p_1 = \sum_{m=0}^{K-1} \pi_m q_m$. Similarly, the stationary probability of the encoder outputting a bit '0' can be calculated by $p_0 = \sum_{m=0}^{K-1} \pi_m (1 - q_m)$. Therefore, after the imperfect transmission of the BSC, the probability of bit '1' being received by the SWIPT receiver, which is also the average energy harvested from a single received bit is expressed as

$$E(\widehat{\mathbb{Y}}) = p_1(1-\omega) + p_0\omega = \sum_{m=0}^{K-1} \pi_m [q_m(1-\omega) + (1-q_m)\omega]. \tag{9}$$

which is a function of the codeword distribution $\mathbf{P}$, since $\{q_m | 0 \leq m \leq K-1\}$ are all functions of $\mathbf{P}$, according to Eq.(2). The entries in $\boldsymbol{\pi}$ are also functions of $\mathbf{P}$, according to Eq.(4).

B. Finite Battery Capacity

When the battery has a finite capacity $B_{\max}$, we study the battery overflow probability p_{of} at the SWIPT receiver. Furthermore, we define a warning threshold $B_{\min}$, which is the minimum required energy for supporting the routine operation of the SWIPT receiver. Therefore, we also study the battery underflow probability p_{uf}.

The instantaneous energy level can be modelled by the following queuing process:

$$B(t+1) = \begin{cases} \min\{B_{\min}, B(t) + \lambda(t) - \mu(t)\}, \\ \max\{B(t) + \lambda(t) - \mu(t), B_{\max}\}, \end{cases} \tag{10}$$

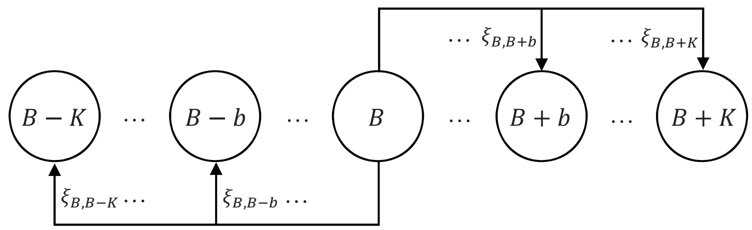

Fig. 4. Markov modelling of the battery queuing process $B(t)$.

where $B(t)$ is the energy level of the battery at the t-th instant, $\lambda(t)$ is the amount of energy arriving at the battery of the SWIPT receiver at the t-th instant and $\mu(t)$ is the amount of energy departing from the battery at the t-th instant. The energy level $B(t+1)$ at the $(t+1)$-th instant is lower-bounded by $B_{\min}$ and upper-bounded by the finite capacity $B_{\max}$. For a single instant considered, an arbitrary unary codeword is sent by the SWIPT transmitter.

Specifically, the energy arrival $\lambda(t)$ is a stochastic process, which has the following randomness:

- A codeword $\mathcal{X}_j$ is randomly sent by the SWIPT transmitter with a probability of $p(\mathcal{X}_j)$, which originally conveys $(j-1)$ energy unit.
- The bits in the codeword $\mathcal{X}_j$ may be randomly flipped by the BSC.

We assume that the probability of the SWIPT receiver consuming a single energy unit in a bit duration is ν. Therefore, if a codeword $\mathcal{X}_j$ is sent by the SWIPT transmitter at the t-th instant, the amount of energy $\mu(t)$ consumed by the SWIPT receiver is a Binomial distributed random variable having parameters of (j, ν).

The queuing process $B(t)$ can be further modelled by another discrete Markov chain, as illustrated in Fig.4. The states in this Markov chain span from $B_{\min}$ to $B_{\max}$, which represent all possible energy levels of the battery. We now study the state transition probabilities of this Markov chain at a single instant, which is also the duration of a unary codeword. The probability of the energy level increment $b = \lambda(t) - \mu(t)$ is defined as ξ_b, which is expressed as

$$\begin{aligned}\xi_b &= \sum_{\mathcal{X}_j} \sum_{\lambda} p(\mu(t) = \lambda(t) - b, \lambda(t) = \lambda, \mathcal{X}_j) \\ &= \sum_{j=1}^{K} p(\mathcal{X}_j) \sum_{\lambda} p(\mu(t) = \lambda - b | \lambda(t) = \lambda, \mathcal{X}_j) p(\lambda(t) = \lambda | \mathcal{X}_j)\end{aligned} \tag{11}$$

Given the unary codeword $\mathcal{X}_j$ sent at the t-th instant, the conditional probability of $\lambda(t) = \lambda$ is expressed as

$$p(\lambda(t) = \lambda | \mathcal{X}_j) = \begin{cases} \binom{j}{\lambda} \dfrac{(1-\omega)^{\lambda-1}\omega^{j-1-\lambda}}{j} \left[(j-\lambda)(1-\omega)^2 + \lambda\omega^2\right], & 0 \le \lambda \le j, \\ 0, & \text{otherwise.} \end{cases} \tag{12}$$

Given the unary codeword $\mathcal{X}_j$ and $\lambda(t) = \lambda$, the conditional probability $p(\mu(t) = \lambda - b | \mathcal{X}_j, \lambda(t) = \lambda)$ is calculated as

$$p(\mu(t) = \lambda - b | \mathcal{X}_j, \lambda(t) = \lambda) = \begin{cases} \binom{j}{\lambda - b} \nu^{\lambda-b}(1-\nu)^{j-\lambda+b}, & 0 \le \lambda - b \le j, \\ 0, & \text{otherwise.} \end{cases} \tag{13}$$

By substituting both Eqs.(12) and (13) into (11), we may obtain ξ_b as

$$\xi_b = \sum_{j=1}^{2^k} p(\mathcal{X}_j)\Phi(b, j), \text{ for } -2^k \le b \le 2^k, \tag{14}$$

otherwise, $\xi_b = 0$, where we have

$$\Phi(b, j) = \begin{cases} \displaystyle\sum_{\lambda=b}^{j} \binom{j}{\lambda - b}\binom{j}{\lambda} \nu^{\lambda-b}(1-\nu)^{j-\lambda+b} \frac{(1-\omega)^{\lambda-1}\omega^{j-1-\lambda}}{j} \left[(j-\lambda)(1-\omega)^2 + \lambda\omega^2\right], & 0 \le b \le j, \\ \displaystyle\sum_{\lambda=0}^{j+b} \binom{j}{\lambda - b}\binom{j}{\lambda} \nu^{\lambda-b}(1-\nu)^{j-\lambda+b} \frac{(1-\omega)^{\lambda-1}\omega^{j-1-\lambda}}{j} \left[(j-\lambda)(1-\omega)^2 + \lambda\omega^2\right], & -j \le b \le 0, \\ 0, & \text{otherwise,} \end{cases} \tag{15}$$

Without loss of generality, we assume that the battery has an energy level of $B(t) = B$ at the t-th instant. Therefore, at the $(t + 1)$-th instant, the energy level of the battery could be $B(t+1) = B+b$, which also represents the state transition from B to $(B+b)$ in the Markov chain of Fig.4. The corresponding state transition probability $\xi_{B,B+b}$ can be then expressed as

$$\xi_{B,B+b} = \begin{cases} \xi_b, & \max(B_{\min} - B + 1, -K) \leq b \leq \min(B_{\max} - B - 1, K) \\ & \text{and } B_{\min} + 1 \leq B \leq B_{\max} - 1, \\ 0, & K < b \leq B_{\max} - B \text{ and } B_{\min} \leq B < B_{\max} - K, \\ 0, & B_{\min} - B \leq b < -K \text{ and } B_{\min} + K < B \leq B_{\max}. \end{cases} \tag{16}$$

If the current energy level B satisfies $B_{\max} - K \leq B \leq B_{\max}$ and the energy level increment b satisfies $B_{\max} - B \leq b \leq K$, the energy level of the battery at the end of this instant is constrained to $B_{\max}$, according to Eq.(10). Therefore, the state transition probability $\xi_{B,B_{\max}}$ is expressed as

$$\xi_{B,B_{\max}} = \sum_{b=B_{\max}-B}^{K} \xi_b, \text{ for } B_{\max} - K \leq B \leq B_{\max}. \tag{17}$$

Similarly, if the current energy level satisfies $B_{\min} \leq B \leq B_{\min}+K$ and the energy level increment b satisfies $-K \leq b \leq B_{\min}-B$, the energy level of the battery at the end of this instant is constrained to $B_{\min}$, according to Eq.(10). Therefore, the state transition probability $\xi_{B,B_{\min}}$ is expressed as

$$\xi_{B,B_{\min}} = \sum_{b=-K}^{B_{\min}-B} \xi_b, \text{ for } B_{\min} \leq B \leq B_{\min} + K. \tag{18}$$

With the aid of Eqs.(16)-(18), the state transition probability matrix $\mathbf{\Xi} = [\xi_{i,j}]$ is found. By following the similar method of Eq.(4), the stationary distribution $\widehat{\boldsymbol{\pi}} = \{\widehat{\pi}_{B_{\min}}, \cdots, \widehat{\pi}_B, \cdots, \widehat{\pi}_{B_{\max}}\}$ is obtained for all the states in the Markov chain of Fig.4. Finally, the battery overflow probability p_{of} and the underflow probability p_{uf} are then formulated as

$$\begin{cases} p_{of} = \displaystyle\sum_{B=B_{\max}-K+1}^{B_{\max}} \widehat{\pi}_B \sum_{b=B_{\max}-B+1}^{K} \xi_b, \\ p_{uf} = \displaystyle\sum_{B=B_{\min}}^{B_{\min}+K-1} \widehat{\pi}_B \sum_{b=-K}^{B_{\min}-B-1} \xi_b, \end{cases} \tag{19}$$

According to Eq.(14), both p_{of} and p_{uf} are the functions of the codeword distribution $\mathbf{P}$.

V. Optimal Coding Design

A. Problem Formulation

We formulate the first optimal coding design by considering an infinite battery capacity at the SWIPT receiver, when the 2^k-level unary code is adopted at the SWIPT transmitter:

$$\text{(P1):} \ \max_{\mathbf{P}} E(\widehat{\mathbb{Y}}), \tag{20}$$

$$\text{s. t.:} \ I_{\inf}(\widehat{\mathbb{X}}; \widehat{\mathbb{Y}}) \geq R_{th}. \tag{20a}$$

The objective of (P1) is to maximise the average energy $E(\widehat{\mathbb{Y}})$ of Eq.(9) harvested from a single received bit by finding the optimal codeword distribution $\mathbf{P}_1^*$, while satisfying the constraint (20a) that the mutual information's infinimum $I_{\inf}(\widehat{\mathbb{X}}; \widehat{\mathbb{Y}})$ of Eq.(8) should be higher than a rate threshold R_{th}. Since we have $R = I(\widehat{\mathbb{X}}; \widehat{\mathbb{Y}}) \geq I_{\inf}(\widehat{\mathbb{X}}; \widehat{\mathbb{Y}})$, the actual information transmission rate R is also higher than R_{th}.

We then formulate the second optimal coding design by considering a finite battery capacity at the SWIPT receiver:

$$\text{(P2):} \ \min_{\mathbf{P}} p_{of}(\text{or } p_{uf}), \tag{21}$$

$$\text{s. t.:} \ I_{\inf}(\widehat{\mathbb{X}}; \widehat{\mathbb{Y}}) \geq R_{th}. \tag{21a}$$

In contrast to (P1), we aim for minimising the battery's overflow or underflow probabilities in (P2) by finding the optimal codeword distribution $\mathbf{P}_2^*$, while satisfying the minimum rate requirement R_{th}.

B. ES Aided Coding Design

The calculations of $I_{\inf}(\widehat{\mathbb{X}}; \widehat{\mathbb{Y}})$ and $E(\widehat{\mathbb{Y}})$ as well as p_{of} and p_{uf} all require the stationary distribution $\boldsymbol{\pi}$, which may only be obtained by numerically solving the system of linear equations

Algorithm 1 ES algorithm for solving (P1)

Input: The crossover probability ω of the BSC; The probability increment ε for the ES; The minimum WIT requirement R_{th};
Output: The optimal codeword distribution $\mathbf{P}_1^*$; The maximum average energy carried per received bit $E_{\max}(\widehat{\mathbb{Y}})$;

Initialise a K-dimensional probability space for the exhaustive search: $\mathcal{P} \leftarrow \{m\varepsilon | m = 0, 1, \cdots, \lfloor 1/\varepsilon \rfloor\}^K$;
Initialise $E_{\max} \leftarrow 0$;
while $\mathcal{P}$ is not null **do**
  Let $\mathbf{P}_1 \leftarrow$ an arbitrary $K \times 1$ vector from $\mathcal{P}$;
  Calculate $I_{\inf}(\widehat{\mathbb{X}}; \widehat{\mathbb{Y}})$ by substituting $\mathbf{P}_1$ into (8);
  if $I_{\inf}(\widehat{\mathbb{X}}; \widehat{\mathbb{Y}}) \geq R_{th}$ **then**
    Calculate $E(\widehat{\mathbb{Y}})$ by substituting $\mathbf{P}_1$ into (9);
    if $E(\widehat{\mathbb{Y}}) > E_{\max}$ **then**
      Let $E_{\max} \leftarrow E(\widehat{\mathbb{Y}})$ and $\mathbf{P}_1^* = \mathbf{P}_1$;
    end if
  end if
  Let $\mathcal{P} \leftarrow \mathcal{P} - \mathbf{P}_1$;
end while
return $E_{\max}(\widehat{\mathbb{Y}}) \leftarrow E_{\max}$ and $\mathbf{P}_1^*$.

(4), given a specific state transition probability matrix $\mathbf{Q}$. Therefore, the optimisation problems (P1) and (P2) cannot be solved in polynomial time, when we have a high-level unary encoder.

We first provide an exhaustive searching (ES) based algorithm for solving the optimisation problem (P1), whose pseudo code is provided in Algorithm 1. Its complexity $O(\lfloor 1/\varepsilon \rfloor^K)$ depends on the searching increment ε. If we increase ε for obtaining a more accurate result, the complexity increases dramatically. Furthermore, Algorithm 1 can also be slightly adjusted for solving (P2), which is omitted here for the page limitation.

C. GA Aided Coding Design

In order to reduce the computing complexity of the coding design but maintain its optimality, we then propose a GA aided coding design for solving the optimisation problem (P2). By exploiting both hybrid and mutation treatments on the 'parents', GA aided coding design is capable of escaping from the local optimum, which is detailed in Algorithm 2. The main steps of Algorithm 2 can be summarised as below:

- *Step 1*: Randomly generate N legitimate codeword distribution as a generation $\mathcal{P}$, as shown in Line 1 of Algorithm 2.

- *Step 2*: Calculate corresponding mutual information, overflow probabilities and the survival probabilities for all the codeword distributions in $\mathcal{P}$, as detailed in Lines 4-15 of Algorithm 2, while update the minimum overflow probability $p_{of,\min}$, as shown in Lines 16-18 of Algorithm 2. If the mutual information of an individual codeword distribution violates the minimum rate requirement R_{th}, its corresponding overflow probabilities are set to 1. According to Line 14, this individual has a zero survival probability.
- *Step 3*: Randomly select individuals from $\mathcal{P}$ according to their survival probabilities $\mathbf{p}_{live}$ in order to generate the parental individuals $\mathcal{P}_{sel}$ for the sake of giving birth to the next generation, as detailed in Lines 19-26 of Algorithm 2. The individuals having lower overflow probabilities can be selected with higher probabilities.
- *Step 4*: Obtain new generation $\mathcal{P}'$ by carrying out cross over and mutation on the parental individuals $\mathcal{P}_{sel}$ in Algorithm 3 and repeat from Step 2. Finally, we may obtain the minimum overflow probability $p_{of,\min}$ and the optimal codeword distribution $\mathbf{P}_2^*$.

Furthermore, Algorithm 3 provides the details of crossover and mutation operations on the parental individuals. All the N child individuals are born by the crossover of a randomly chosen parents from $\mathcal{P}_{sel}$, as shown in Lines 2-4 of Algorithm 3. Every child individual has a probability of ε to mutate, as illustrated in Lines 5-13 of Algorithm 3. Specifically, Lines 8-11 ensures that the mutated individual is a legitimate codeword distribution.

The complexity of the proposed GA aided optimal coding design is $O(G^2)$, where G is the number of generations in Algorithm 2. The complexity is irrelevant to the level K of the unary code. Therefore, when a high-level unary code is adopted for the SWIPT, the GA aided optimal coding design is capable of substantially reducing the computational complexity. Furthermore, by substituting p_{of} in Algorithm 2 by p_{uf}, we can readily obtain the optimal codeword distribution for minimising the underflow probability. Furthermore, Algorithm 2 can also be slightly adjusted for solving (P1), which is omitted here for the page limitation.

Algorithm 2 GA aided optimal coding design for solving the optimisation problem (P2)

Input: The crossover probability ω of the BSC; The minimum WIT requirement R_{th}; The maximum number of generations G; The population of a single generation N;
Output: The minimum overflow probabilities $p_{of,\min}$; The optimal codeword distribution $\mathbf{P}_2^*$;

Randomly initialise a generation $\mathcal{P} \leftarrow \{\mathbf{P}_{(j)} | j = 1, \cdots, N\}$, where $\mathbf{P}_{(j)}$ is a legitimate codeword distribution;
Initialise a generation index $g \leftarrow 1$ and the minimum overflow probability $p_{of,\min} \leftarrow 1$;
while $g \leq G$ **do**
  Initialise the mutual information of the g-th generation $\mathcal{I} \leftarrow \{I_{\inf,(j)} | j = 1, \cdots, N\}$, where $I_{\inf,(j)}$ is calculated by substituting $\mathbf{P}_{(j)}$ into Eq.(8);
  Initialise the overflow probabilities of the g-th generation $\mathbf{p}_{of} \leftarrow \{p_{of,(j)} \leftarrow 1 | j = 1, \cdots, N\}$;
  Initialise the survival probabilities of the g-th generation $\mathbf{p}_{live} \leftarrow \{p_{live,(j)} \leftarrow 0 | j = 1, \cdots, N\}$;
  Initialise the selected parental individuals $\mathcal{P}_{sel} \leftarrow \{\mathbf{P}_{sel,(j)} \leftarrow \mathbf{P}_{(j)} | j = 1, \cdots, N\}$;
  for $\forall j = 1, \cdots, N$ **do**
    if $I_{\inf,(j)} \geq R_{th}$ **then**
      Update $p_{of,(j)}$ by substituting $\mathbf{P}_{(j)}$ into Eq.(19);
    else
      Update $p_{of,(j)} \leftarrow 1$;
    end if
    Update $p_{live,(j)} \leftarrow \dfrac{(1 - p_{of,(j)})}{\sum_j (1 - p_{of,(j)})}$;
  end for
  if $\min \mathbf{p}_{of} < p_{of,\min}$ **then**
    Update $p_{of,\min} \leftarrow \min \mathbf{p}_{of}$;
  end if
  for $\forall j = 1, \cdots, N$ **do**
    Generate ζ uniformly distributed in $[0, 1]$;
    Initialise a temporary index $n \leftarrow 1$;
    while $\zeta - p_{\text{live},(n)} \geq 0$ **do**
      Update $\zeta \leftarrow \zeta - p_{live,(n)}$ and $n \leftarrow n + 1$;
    end while
    Update $\mathbf{P}_{sel,(j)} \leftarrow \mathbf{P}_{(n)}$;
  end for
  Obtain a new generation $\mathcal{P}'$ by inputting $\mathcal{P}_{sel}$ into Algorithm 3 and update $\mathcal{P} \leftarrow \mathcal{P}'$;
end while
return $p_{of,\min}$ and $\mathbf{P}_2^*$.

Algorithm 3 Crossover and mutation algorithm

Input: A selected parental individuals $\mathcal{P}_{sel}$; A mutation probability ε.
Output: A new generation $\mathcal{P}'$;

Initialise a new generation $\mathcal{P}' \leftarrow \{\mathbf{P}'_{(j)} \leftarrow \mathbf{P}_{sel,(j)} | j = 1, \cdots, N\}$;
for $\forall j = 1, \cdots, N$ **do**
  Randomly choose a pair of individuals $\mathbf{P}_{sel,(m)}$ and $\mathbf{P}_{sel,(l)}$ from $\mathcal{P}_{sel}$;
  Update $\mathbf{P}'_{(j)} \leftarrow \dfrac{\mathbf{P}_{sel,(m)} + \mathbf{P}_{sel,(l)}}{2}$;
  Generate ζ uniformly distributed in $[0, 1]$;
  if $\zeta \leq \varepsilon$ **then**
    Update $\mathbf{P}'_{(j)} \leftarrow \mathbf{P}'_{(j)} + \boldsymbol{\gamma}$, where $\boldsymbol{\gamma} \sim \mathcal{N}(0, \mathbf{I}) \in \mathcal{R}^{1 \times K}$;
    if $\min \mathbf{P}'_{(j)} < 0$ **then**
      Update $\mathbf{P}'_{(j)} \leftarrow \mathbf{P}'_{(j)} - \min \mathbf{P}'_{(j)}$;
    end if
    Normalise $\mathbf{P}'_{(j)} \leftarrow \mathbf{P}'_{(j)} / \sum \mathbf{P}'_{(j)}$;
  end if
end for
return $\mathcal{P}'$.

VI. Numerical Results

In this section, we characterise the performance of the unary coded SWIPT system by providing a range of numerical results.

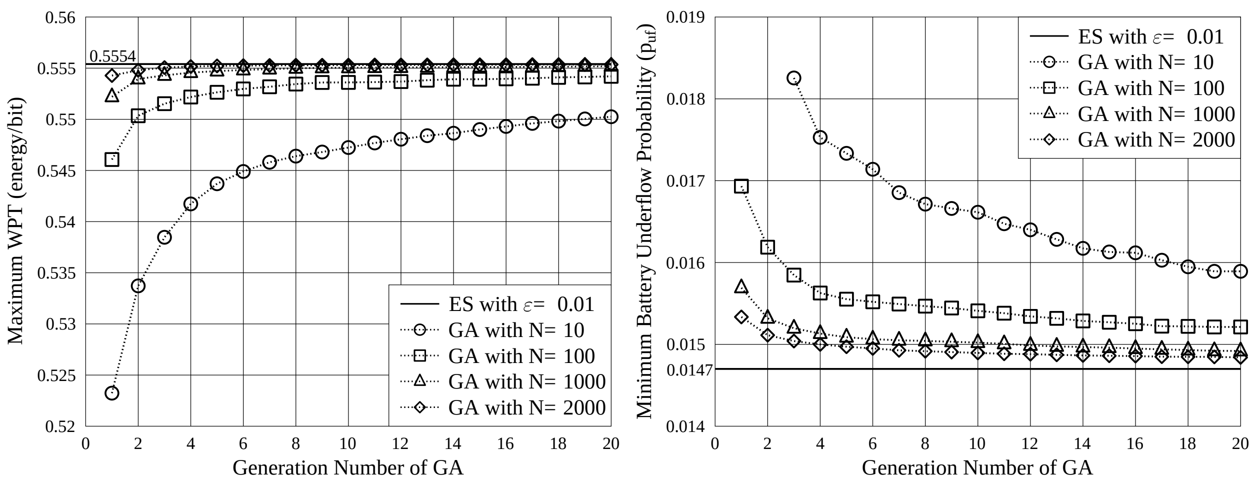

(a) (b)

Fig. 5. Convergence of the GA aided coding design with different population $N = \{10, 100, 1000, 2000\}$, where the 4-level unary code is adopted, the cross over probability of the BSC is $\omega = 0.2$ and the minimum WIT requirement is $R_{th} = 0.22$ bit: (a) The maximum WPT performance $E_{\max}(\mathbb{Y})$ with infinite battery capacity and (b) the minimum underflow probability $p_{\min,uf}$ with finite battery capacity.

A. *GA vs ES*

First of all, we demonstrate the convergence of the GA aided coding design and compare its performance to that of the ES aided counterpart in Fig.5. All the performance of Fig.5 is attained by averaging over 50 random results. Observe from Fig.5 that the GA aided coding design converges to the optimality in terms of both $E_{\max}(\mathbb{Y})$ and $p_{\min,uf}$, as the generation number increases. Furthermore, as shown in Fig.5(a), the GA aided coding design with medium population $N = 100$ converges after only 10 generations. The maximum WPT attained is around $E_{\max}(\mathbb{Y}) = 0.5536$ energy/bit, only 0.3% lower than that of the ES aided counterpart. However, as shown in Fig.5(b), the minimum underflow probability of the GA aide coding design converges a little slow. The minimum underflow probability $p_{\min,uf} = 0.0152$ attained by the GA with $N = 100$ after 20 generations is 3.5% higher than that of the ES aided counterpart. Since the low-complexity GA aided coding design achieves almost the same performance with the ES, the rest of the simulation results are obtained by invoking GA.

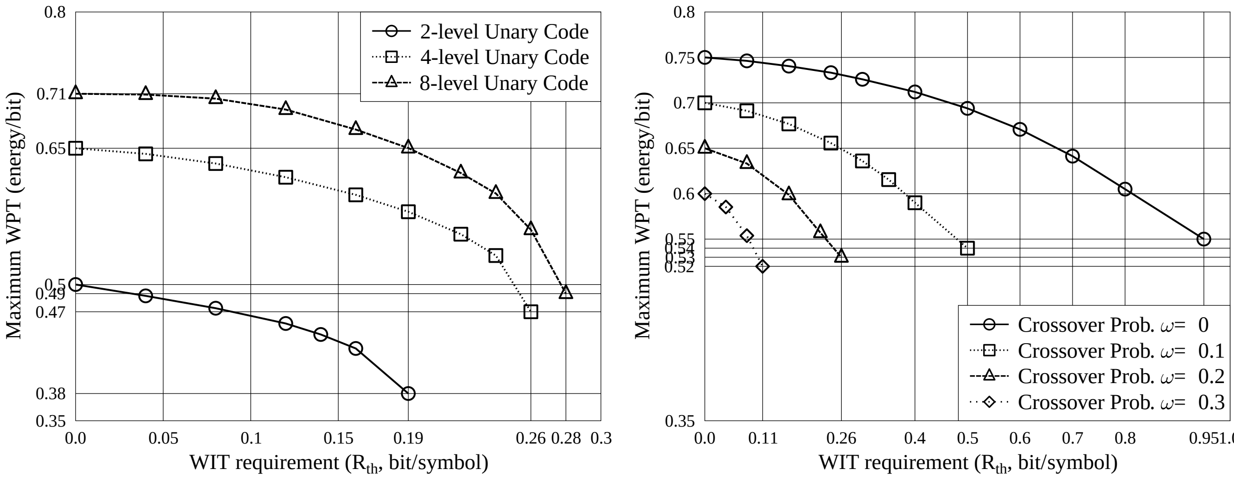

(a) (b)

Fig. 6. The SWIPT performance with an infinite battery capacity: (a)(2,4,8)-level unary codes in the BSC of $\omega = 0.2$; (b) 4-level unary code in the BSC of $\omega = \{0.3, 0.2, 0.1, 0\}$.

B. Infinite Battery Capacity

We then investigate the SWIPT performance by considering an infinite battery capacity in Fig.6, where the WPT performance is characterised by the average number of energy units carried by a single received bit. Observe from both Figs.6(a) and (b) that the maximum WPT performance $E_{\max}(\mathbb{Y})$ reduces, as we increase the WIT requirement R_{th}. Note that R_{th} cannot exceed the channel capacity due to the limited WIT capability of a specific. For instance, as illustrated in Fig.6(a), the maximum WIT capability of 2-level unary code is 0.19 bit/symbol. When we have $R_{th} = 0.19$ bit/symbol, the WPT performance reaches its lowest. We may further observe from Fig.6(a) that the 8-level unary code has supreme SWIPT performance. As portrayed in Fig.6, when the BSC becomese better, as we reduce the crossover probability ω, the SWIPT performance of the 4-level unary code is improved.

C. Finite Battery Capacity

We finally investigate the SWIPT performance by considering a finite battery capacity in Fig.7. Observe from Figs.7(a) and (d) that both the battery overflow and underflow probabilities are

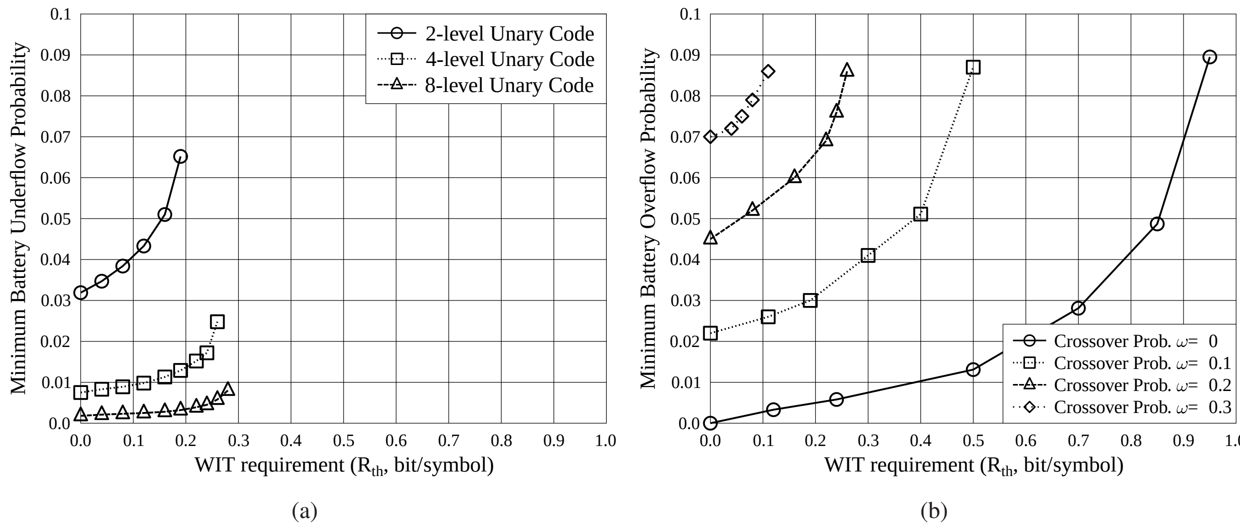

Fig. 7. The SWIPT performance with a finite battery capacity $B_{\max} = 2$ and $B_{\min} = 0$, while the receiver may consume an energy unit with a probability of $\nu = 0.5$: (a) (2,4,8)-level unary codes in the BSC of $\omega = 0.2$ of the BSC; (b) 4-level unary code in the BSC of $\omega = \{0.3, 0.2, 0.1, 0\}$.

increased, as the WIT requirement becomes stringent. Since the unary codeword distribution has to be adjusted in order to satisfy the harsh WIT requirement, the battery overflow and underflow probabilities are inevitably sacrificed during the coding design. Furthermore, as illustrated in Fig.7(a), a higher level of unary code has higher freedom for the sake of satisfying harsher WIT requirements and reaching better WPT performance. Moreover, observe from Fig.7 when the BSC becomes worse, as the crossover probability ω increases, the SWIPT performance of the unary code is also degraded.

VII. Conclusion

A unary coded SWIPT transceiver is studied in this paper by considering a classic BSC. The unary coded transmitter is modelled by a Markov chain having finite states, which is relied upon for the WIT and WPT performance analysis. The optimal codeword distribution is found by exploiting the low-complexity GA for maximising the average energy harvested from a single received bit and for minimising the battery overflow/underflow probability, respectively, by satisfying the minimum requirement of the information transmission rate. The numerical results demonstrates the feasibility of the GA aided coding design and they explicitly characterise the tradeoff between the WIT and the WPT in the coding level.

References

[1] Z. Dawy, W. Saad, A. Ghosh, J. G. Andrews, and E. Yaacoub, "Toward Massive Machine Type Cellular Communications," *IEEE Wireless Communications*, vol. 24, no. 1, pp. 120–128, February 2017.

[2] M. P. R. S. Kiran, V. Subrahmanyam, and P. Rajalakshmi, "Novel Power Management Scheme and Effects of Constrained On-Node Storage on Performance of MAC Layer for Industrial IoT Networks," *IEEE Transactions on Industrial Informatics*, vol. 14, no. 5, pp. 2146–2158, May 2018.

[3] L. Roselli, N. B. Carvalho, F. Alimenti, P. Mezzanotte, G. Orecchini, M. Virili, C. Mariotti, R. GonÃğalves, and P. Pinho, "Smart Surfaces: Large Area Electronics Systems for Internet of Things Enabled by Energy Harvesting," *Proceedings of the IEEE*, vol. 102, no. 11, pp. 1723–1746, Nov 2014.

[4] K. Yang, Q. Yu, S. Leng, B. Fan, and F. Wu, "Data and Energy Integrated Communication Networks for Wireless Big Data," *IEEE Access*, vol. 4, pp. 713–723, 2016.

[5] M. Manoufali, K. Bialkowski, B. Mohammed, and A. Abbosh, "Wireless Power Link Based on Inductive Coupling for Brain Implantable Medical Devices," *IEEE Antennas and Wireless Propagation Letters*, vol. 17, no. 1, pp. 160–163, Jan 2018.

[6] H. H. Lee, S. H. Kang, and C. W. Jung, "MR-WPT With Reconfigurable Resonator and Ground for Laptop Application," *IEEE Microwave and Wireless Components Letters*, vol. 28, no. 3, pp. 269–271, March 2018.

[7] J. Hu, K. Yang, G. Wen, and L. Hanzo, "Integrated Data and Energy Communication Network: A Comprehensive Survey," *IEEE Communications Surveys Tutorials, early access*, August 2018.

[8] B. Clerckx and E. Bayguzina, "Waveform Design for Wireless Power Transfer," *IEEE Transactions on Signal Processing*, vol. 64, no. 23, pp. 6313–6328, Dec 2016.

[9] Y. Zeng, B. Clerckx, and R. Zhang, "Communications and Signals Design for Wireless Power Transmission," *IEEE Transactions on Communications*, vol. 65, no. 5, pp. 2264–2290, May 2017.

[10] X. Zhou, R. Zhang, and C. K. Ho, "Wireless Information and Power Transfer: Architecture Design and Rate-Energy Tradeoff," *IEEE Transactions on Communications*, vol. 61, no. 11, pp. 4754–4767, November 2013.

[11] R. Zhang and C. K. Ho, "MIMO Broadcasting for Simultaneous Wireless Information and Power Transfer," *IEEE Transactions on Wireless Communications*, vol. 12, no. 5, pp. 1989–2001, May 2013.

[12] K. Lv, J. Hu, Q. Yu, and K. Yang, "Throughput Maximization and Fairness Assurance in Data and Energy Integrated Communication Networks," *IEEE IoT Journal*, vol. 5, no. 2, pp. 636–644, April 2018.

[13] J. Yang, J. Hu, K. Lv, Q. Yu, and K. Yang, "Multi-Dimensional Resource Allocation for Uplink Throughput Maximisation in Integrated Data and Energy Communication Networks," *IEEE Access*, vol. 6, pp. 47 163–47 180, 2018.

[14] Y. Zhao, J. Hu, Y. Diao, Q. Yu, and K. Yang, “Modelling and Performance Analysis of Wireless LAN Enabled by RF Energy Transfer,” *IEEE Transactions on Communications*, vol. 66, no. 11, pp. 5756–5772, Nov 2018.

[15] Y. Zhao, J. Hu, R. Guo, K. Yang, and S. Leng, “Enhanced CSMA/CA Protocol Design for Integrated Data and Energy Transfer in WLANs,” in *proceedings of IEEE Globecom 2018*, Dec 2018.

[16] Y. Zhao, D. Wang, J. Hu, and K. Yang, “H-AP Deployment for Joint Wireless Information and Energy Transfer in Smart Cities,” *IEEE Transactions on Vehicular Technology*, vol. 67, no. 8, pp. 7485–7496, Aug 2018.

[17] L. R. Varshney, “Transporting Information and Energy Simultaneously,” in *2008 IEEE ISIT*, Jul. 2008, pp. 1612–1616.

[18] ——, “On Energy/Information Cross-Layer Architectures,” in *2012 IEEE International Symposium on Information Theory Proceedings*. IEEE, Jul 2012, pp. 1356–1360.

[19] A. Tandon, M. Motani, and L. R. Varshney, “Subblock-Constrained Codes for Real-Time Simultaneous Energy and Information Transfer,” *IEEE Trans. on Info. Theory*, vol. 62, no. 7, pp. 4212–4227, Jul 2016.

[20] A. I. Barbero, E. Rosnes, G. Yang, and O. Ytrehus, “Constrained codes for passive RFID communication,” in *2011 IEEE ITA*, Feb. 2011, pp. 1–9.

[21] A. M. Fouladgar, O. Simeone, and E. Erkip, “Constrained Codes for Joint Energy and Information Transfer,” *IEEE Trans. on Comm.*, vol. 62, no. 6, pp. 2121–2131, Jun. 2014.

[22] A. Tandon, M. Motani, and L. R. Varshney, “On Code Design for Simultaneous Energy and Information Transfer,” in *2014 Information Theory and Applications Workshop (ITA)*. IEEE, feb 2014, pp. 1–6. [Online]. Available: http://ieeexplore.ieee.org/document/6804257/

[23] Z. Babar, M. A. M. Izhar, H. V. Nguyen, P. Botsinis, D. Alanis, D. Chandra, S. X. Ng, R. G. Maunder, and L. Hanzo, “Unary-Coded Dimming Control Improves ON-OFF Keying Visible Light Communication,” *IEEE Trans. on Comm.*, vol. 66, no. 1, pp. 255–264, Jan. 2018.

[24] W. Zhang, Z. Song, M. F. Brejza, T. Wang, R. G. Maunder, and L. Hanzo, “Learning-Aided Unary Error Correction Codes for Non-Stationary and Unknown Sources,” *IEEE Access*, vol. 4, pp. 2408–2428, 2016.

[25] W. Zhang, M. F. Brejza, T. Wang, R. G. Maunder, and L. Hanzo, “Irregular Trellis for the Near-Capacity Unary Error Correction Coding of Symbol Values From an Infinite Set,” *IEEE Transactions on Communications*, vol. 63, no. 12, pp. 5073–5088, Dec 2015.

[26] T. M. Cover and J. A. Thomas, *Elements of Information Theory*, 2nd ed. John Wiley & Sons, Inc., 2006.

[27] J. Hu, M. Li, and K. Yang, “Appendix of Performance Analysis of the Unary Coding aided SWIPT in a Single-User Z-channel,” UESTC, Tech. Rep., October 2018. [Online]. Available: https://pan.baidu.com/s/1iss1wWSVFTWeKWPm-zjWzA